Journal of Sound and Vibration (2002) **249**(5), 899–907
doi:10.1006/jsvi.2001.3931, available online at http://www.idealibrary.com on IDEAL®

OSCILLATION-SLIDING IN A MODIFIED VAN DER POL–DUFFING ELECTRONIC OSCILLATOR

A. Algaba

Department of Mathematics, Escuela Politécnica Superior, University of Huelva, Spain

AND

F. Fernández-Sánchez, E. Freire, E. Gamero and A. J. Rodríguez-Luis

Department of Applied Mathematics II, Escuela Superior de Ingenieros, University of Sevilla, 41092 *Sevilla, Spain. E-mail: estanis@matina.us.es*

(*Received* 27 *November* 2000, *and in final form* 30 *May* 2001)

Some periodic behaviour exhibited by a modified van der Pol–Duffing electronic oscillator near a degenerate Hopf–pitchfork bifurcation have been studied. Numerical continuation of these periodic orbits leads to the appearance of interesting phenomena. After varying one of the characteristics of the oscillator, oscillation-sliding between two periodic régimes is detected. In the region where oscillation-sliding is present, quasiperiodic oscillations (invariant torus), breakdown of the torus and the corresponding resonant periodic orbits are also found.

1. INTRODUCTION

Electronic analogies have played an important role in the development of theories of dynamical systems. The analogies have formed the basis of theoretical problems, whose analysis has provided evidence of non-trivial behaviour.

It is possible to establish an analogy between some electronic and mechanical magnitudes. This analogy allows new dynamical results to be obtained from electronic systems (that sometimes are easier to handle/measure than mechanical ones) which are also present in mechanical systems. In fact, it has been shown by van der Pol that it is possible to hear harmonics and even the chaos.

In the present paper an interesting phenomenon, named oscillation-sliding, is shown. It appears in a modified van der Pol–Duffing electronic oscillator. The detection of oscillation-sliding is made possible by taking advantage of some analytical results about a degenerate Hopf-pitchfork bifurcation (see, for instance, references [1, 2]).

The paper is organized as follows. In section 2, the electronic model under consideration is described. Section 3 is devoted to the explanation of the analytical results that provide zones in the parameter space where complex dynamical behaviour may be expected. The description of oscillation-sliding appears in section 4. Finally, some conclusions are included.

2. THE MODEL

The electronic oscillator considered in this work is shown schematically in Figure 1. It is composed of an *RC*-circuit (conductance G_1 and capacity C_0) and a parallel

0022-460X/02/050899 + 09 $35.00/0

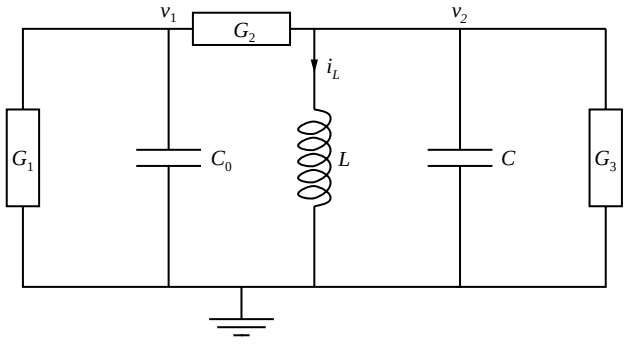

Figure 1. Scheme of the electronic oscillator.

RCL-circuit (conductance G_3, inductance L and capacity C), coupled by means of a conductance G_2.

Taking the voltages on the capacitors and the current across the inductance as variables, the following equations are obtained:

$$C_0 \frac{\mathrm{d}v_1}{\mathrm{d}\tau} = -i_1(v_1) + i_2(v_2 - v_1),$$

$$C \frac{\mathrm{d}v_2}{\mathrm{d}\tau} = -i_L - i_2(v_2 - v_1) - i_3(v_2), \quad L \frac{\mathrm{d}i_L}{\mathrm{d}\tau} = v_2. \tag{1}$$

The current–voltage characteristics of conductance G_j, denoted above by i_j, will be modelled by means of third-degree polynomials as follows:

$$i_1(v) = \mu_1 v + \tilde{A}_3 v^3, \quad i_2(v) = \mu_2 v + \tilde{B}_3 v^3, \quad i_3(v) = \mu_3 v + \tilde{C}_3 v^3. \tag{2}$$

In particular, the current–voltage characteristics are odd functions and thus, the origin is always an equilibrium point.

The present analysis starts by transforming equation (1) into an appropriate form. First, the natural frequency of the oscillation is denoted by $\omega = 1/\sqrt{LC}$. The following dimensionless variables are then introduced: $x = v_1$, $y = v_2$, $z = i_L/\omega C$, and also time and parameters are rescaled by

$$t = \omega\tau, \quad \nu = \frac{\mu_1}{\omega C}, \quad \beta = \frac{\mu_2}{\omega C}, \quad \gamma = \frac{\mu_3}{\omega C},$$

$$r = \frac{C_0}{C}, \quad A_3 = \frac{\tilde{A}_3}{\omega C}, \quad B_3 = \frac{\tilde{B}_3}{\omega C}, \quad C_3 = \frac{\tilde{C}_3}{\omega C}.$$

The equations governing the electronic oscillator can then be written as

$$r\dot{x} = -(\nu + \beta)x + \beta y - A_3 x^3 + B_3(y - x)^3,$$

$$\dot{y} = \beta x - (\beta + \gamma)y - z - B_3(y - x)^3 - C_3 y^3, \quad \dot{z} = y. \tag{3}$$

Note that the parameter r, which represents the ratio of the two capacitors, must always be positive.

The equilibrium at the origin exhibits a diversity of local bifurcations. Among these, a pitchfork bifurcation (see reference [3]) and also Hopf and Takens-Bogdanov bifurcations (analyzed in reference [4]) can be found.

3. REDUCTION TO NORMAL FORM

The present analysis will focus on the study of the Hopf–pitchfork bifurcation of the origin, which occurs when the parameters satisfy $\nu + \beta = 0$, $\beta + \gamma = 0$, $|\gamma| < \sqrt{r}$. The eigenvalues of the linearization matrix at the origin are $\pm i\omega_0$ and 0, with $\omega_0^2 = (r - \gamma^2)/r$.

As this bifurcation is of co-dimension two, ν and β are taken as bifurcation parameters and γ (with $\gamma^2 < r$) is kept fixed.

The normalization of this bifurcation problem has been carried out in reference [5]. In that paper, it is shown that, by taking $\nu \approx \gamma$, $\beta \approx -\gamma$ and changing the state variables and the time, equation (3) can be reduced to the following third order normal form in cylindrical co-ordinates:

$$\begin{aligned} \dot{\rho} &= \rho(\varepsilon_1 + a_{11}\rho^2 + a_{12}z^2) \\ \dot{z} &= z(\varepsilon_2 + a_{21}\rho^2 + a_{22}z^2), \quad \dot{\theta} = \omega_0 + b_1\rho + b_2 z, \end{aligned} \tag{4}$$

where

$$\begin{aligned} \varepsilon_1 &= \frac{\gamma^2(1+r) - r^2}{2r(r-\gamma^2)}(\beta + \gamma) + \frac{\gamma^2}{2r(r-\gamma^2)}(\nu - \gamma), \\ \varepsilon_2 &= -\frac{1}{r-\gamma^2}(\beta + \gamma) - \frac{1}{r-\gamma^2}(\nu - \gamma), \\ a_{11} &= \frac{3(\gamma^4(A_3 + B_3) - (B_3 + C_3)r^2(r-\gamma^2)^2)}{8r^3(r-\gamma^2)}, \\ a_{12} &= \frac{3(\gamma^2(A_3 + B_3) - rB_3(r-\gamma^2))}{2r(r-\gamma^2)}, \\ a_{21} &= \frac{3(-\gamma^2(A_3 + B_3) - rB_3(r-\gamma^2))}{2r^2(r-\gamma^2)}, \\ a_{22} &= -\frac{A_3 + B_3}{r-\gamma^2}. \end{aligned}$$

In the above expressions, the higher order terms in the parameters have been omitted. Moreover, the expressions for b_1, b_2 are not included for the sake of brevity.

The interaction of stationary and periodic bifurcations leads to interesting phenomena, including quasiperiodic, homoclinic and heteroclinic behaviours (see, for instance, reference [1]). The parameter values where these phenomena occur can be predicted once the normal form (4) has been computed. The analysis is based on the rotational symmetry of the normal form. This property allows the azimuthal component θ to be uncoupled and reduces the study to the bi-dimensional system of variables ρ, z. The two-dimensional flow can be viewed as approximating to a local Poincaré map of the full system when recovering the azimuthal component, so that some of the information achieved can be easily translated to the three-dimensional flow.

Rotating about the z-axis, a correspondence between two- and three-dimensional flows is established. So, equilibria on the z-axis remain equilibria, whilst equilibria outside the z-axis become periodic orbits and periodic solutions turn into invariant tori.

The inclusion of the rotation alone does not explain all the dynamics for systems without rotational symmetry. To understand the dynamics in this case, it is necessary to consider the terms that have been neglected in the truncated normal form (4). The symmetry-breaking effect of these terms leads to new bifurcation phenomena related to the breakdown of the

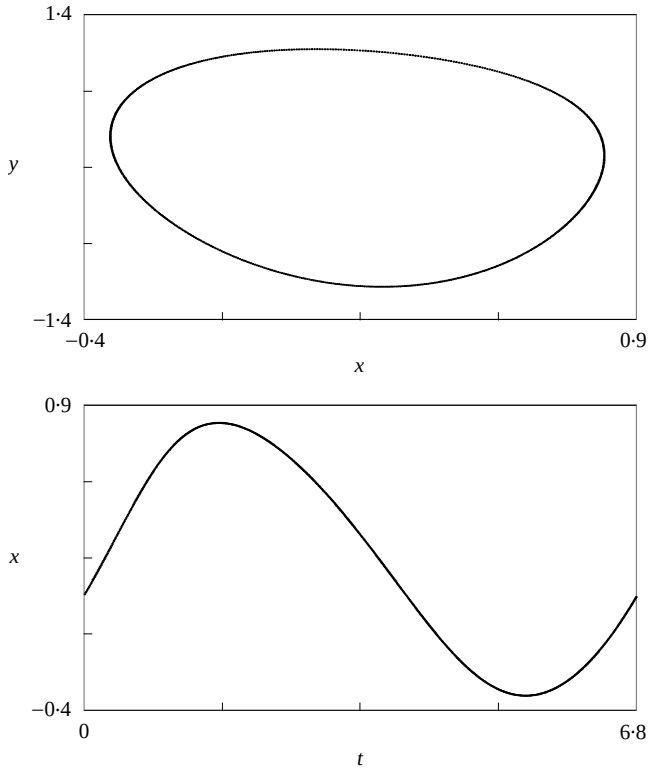

Figure 2. Top: projection onto the xy plane of the periodic orbit corresponding to the parameter values $v = -0{\cdot}5998$, $\beta = 0{\cdot}29254$. Bottom: temporal profile of the periodic orbit (x versus time along a period).

toroidal attractor generated in the secondary Hopf bifurcation of periodic orbits, and also to the homoclinic and heteroclinic connections between equilibria and/or periodic orbits. Moreover, chaotic behaviour is present.

For system (3), several of the above coefficients have a definite sign, namely $a_{21} \leq 0$ and $a_{22} \leqslant 0$. However, different non-linear degeneracies can appear when one of the following equalities holds: $a_{11} = 0$, $a_{12} = 0$ and $\Delta = a_{11}a_{22} - a_{12}a_{21} = 0$ (even more intrincated behaviour appears in these degenerate cases). Here, this last degenerate situation will be considered. To obtain it, system (3) is analyzed with $r = 0{\cdot}6$, $A_3 = 0{\cdot}5$, $B_3 = 0{\cdot}01$ and $C_3 = -0{\cdot}1$. The degenerate case $\Delta = 0$ for the Hopf-pitchfork bifurcation takes place at $\gamma \approx \pm 0{\cdot}2473$. In the following, the negative critical value of γ, $\gamma_c \approx -0{\cdot}2473$, will be considered.

The above analytical information is a useful starting point for the use of adequate numerical tools. In all the numerical work presented here γ will be fixed, as -0.24, close to the critical value γ_c. The aim of this paper is to show some interesting oscillatory behaviour by moving parameters v and β, which is achieved by acting on the linear part of the conductances G_1 and G_2, respectively.

First, fix $\beta = 0{\cdot}29254$. By moving v, it is possible to pass from oscillatory to quasiperiodic motion. In Figure 2, a periodic orbit is shown, for $v = -0{\cdot}5998$ (the program DSTOOL [6] has been used for numerical simulation). This periodic orbit (called principal) undergoes a secondary Hopf bifurcation, giving rise to the appearance of an invariant torus. One of these invariant tori, which occurs for $v = -0{\cdot}5998952$, is shown in Figure 3. Beyond the projection onto the xy plane of the invariant torus, a Poincaré section (cutting off with the

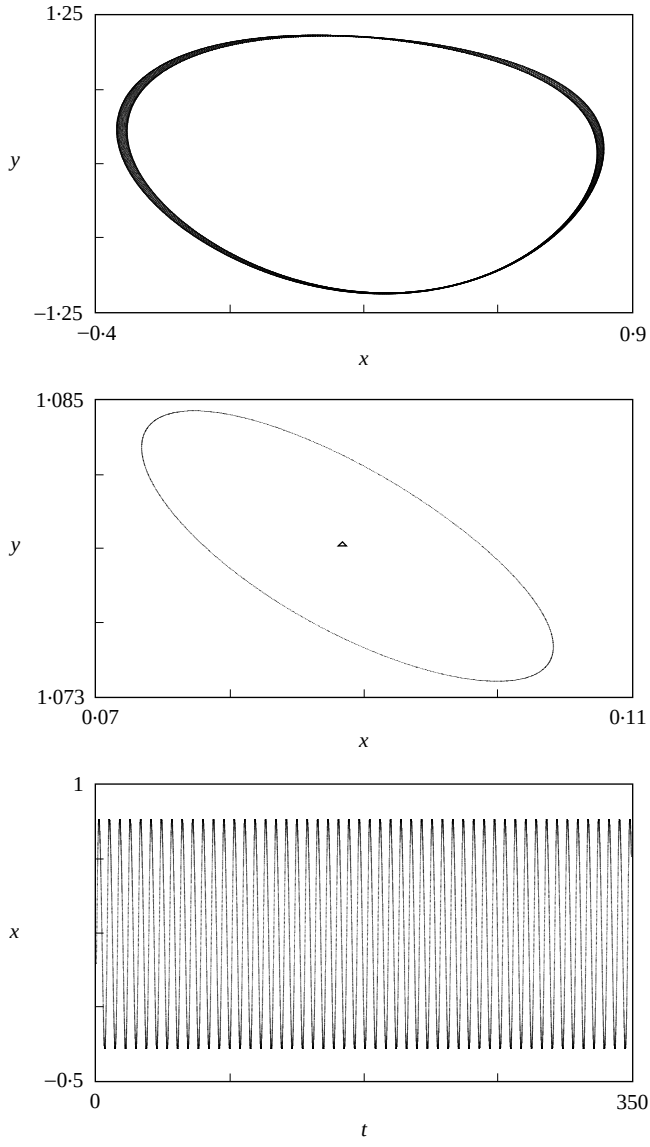

Figure 3. Top: projection onto the xy plane of the invariant torus (quasiperiodic orbit) corresponding to the parameter values $\nu = -0{\cdot}5998952$, $\beta = 0{\cdot}29254$. Middle: Poincaré section of the invariant torus (represented by the closed curve), surrounding the principal periodic orbit (represented by a triangle). Bottom: temporal profile of the quasiperiodic orbit (x versus time).

plane $z = 0$) is included, with the periodic orbit represented by a triangle. The temporal profile of the quasiperiodic behaviour (x versus time) is also shown.

Figure 4 shows the typical situation associated with the breakdown of the invariant torus ($\nu = -0{\cdot}6$), namely, the presence of resonance phenomena leading to phase-locked (also called subharmonic) periodic orbits. In the figure, a Poincaré section (in the plane $z = 0$) appears where the fractal shadow of the torus can be observed. Inside, a pair of 6T periodic orbits, one elliptic and the other hyperbolic (represented by crosses), and the principal periodic orbit (represented by the triangle) can be seen. Outside, a 7T periodic orbit appears. The 6T elliptic periodic orbit is represented in Figure 5.

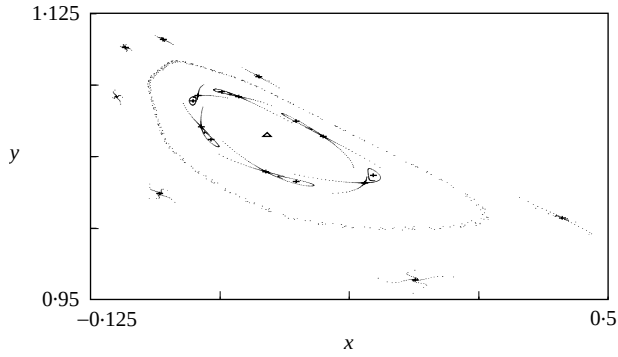

Figure 4. Scenario after the breakdown of the invariant torus corresponding to the parameter values $v = -0{\cdot}6$, $\beta = 0{\cdot}29254$. In the Poincaré section, the fractal shadow of the torus can be observed. Outside, a 7T periodic orbit (represented by crosses) can be seen. Inside, a pair of 6T periodic orbits (elliptic and hyperbolic, both represented by crosses), and the principal periodic orbit (represented by the triangle) appear.

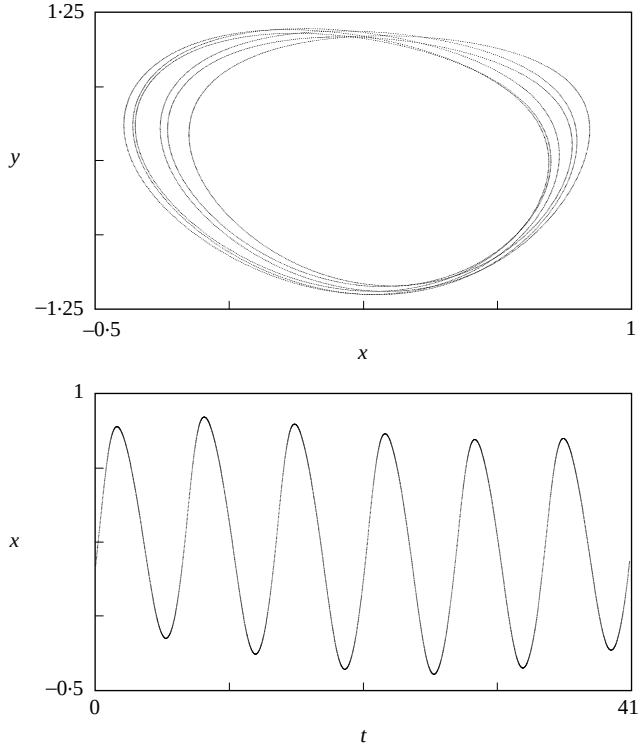

Figure 5. Top: projection onto the xy plane of one 6T periodic orbit corresponding to the parameter values $v = -0{\cdot}6$, $\beta = 0{\cdot}29254$. Bottom: temporal profile of the 6T periodic orbit (x versus time along a period).

The phenomena corresponding to strong resonance is now considered. A 3T periodic orbit, which exists for the values $v = -0{\cdot}75$, $\beta = 0{\cdot}304825$, is represented in Figure 6. A Poincaré section in the plane $z = 0$ of this periodic orbit is also shown (as above, the triangle inside represents the principal periodic orbit).

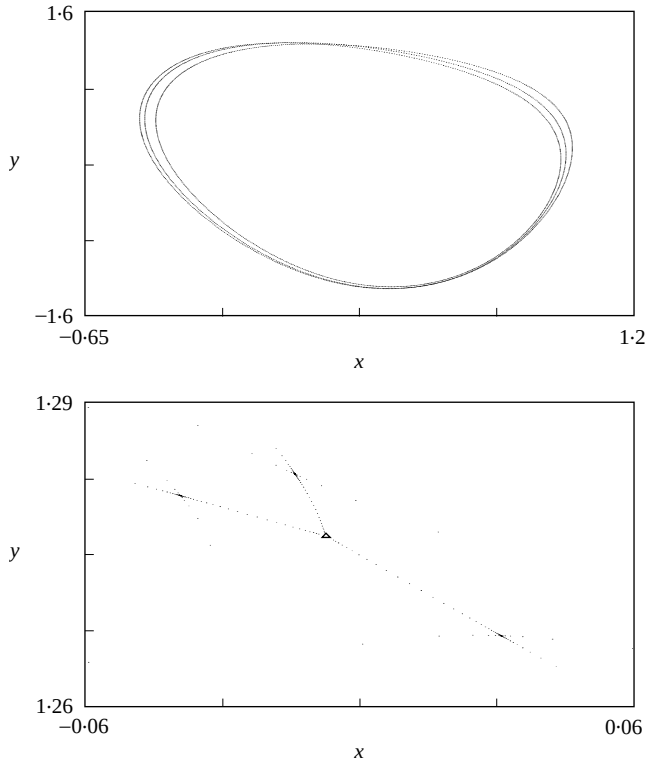

Figure 6. Top: Projection onto the xy plane of the 3T periodic orbit corresponding to the parameter values $v = -0{\cdot}75$, $\beta = 0{\cdot}304825$. Bottom: Poincaré section of the 3T periodic orbit. The triangle in the middle denotes the principal periodic orbit.

Numerical continuation (performed with the AUTO code [7]) of the 3T periodic orbit provides evidence of a new phenomena. This periodic orbit still exists for the value $\beta = 0{\cdot}435$ taking $v \in (-2{\cdot}119680, -1{\cdot}041162)$. As can be seen in Figure 7, the type of oscillations is different when the parameter v is moved.

At the end-points of the interval, the oscillations are of different kinds: large oscillations for $v = -2{\cdot}119680$, and small oscillations for $v = -1{\cdot}041162$. In the middle, the oscillations link the large and the small ones, all the cases being of period 3T. In Figure 7, two of these 3T periodic orbits, corresponding to the values $v = -2{\cdot}045187$ and $v = -1{\cdot}793874$, have also been included.

This phenomenon, referred to as oscillation-sliding (a 3T periodic orbit slides between two different oscillation régimes: a large- and a small-amplitude periodic orbit), is not only present for these 3T periodic orbits but also for other phase-locked periodic orbits on the invariant torus. This fact has been numerically corroborated for 4T, 5T, 6T, 7T, … periodic orbits.

4. CONCLUSIONS

The existence of this phenomenon of oscillation-sliding, that establishes a bridge linking two different periodic régimes, has been identified, taking advantage of some analytical results about a degenerate Hopf–pitchfork bifurcation.

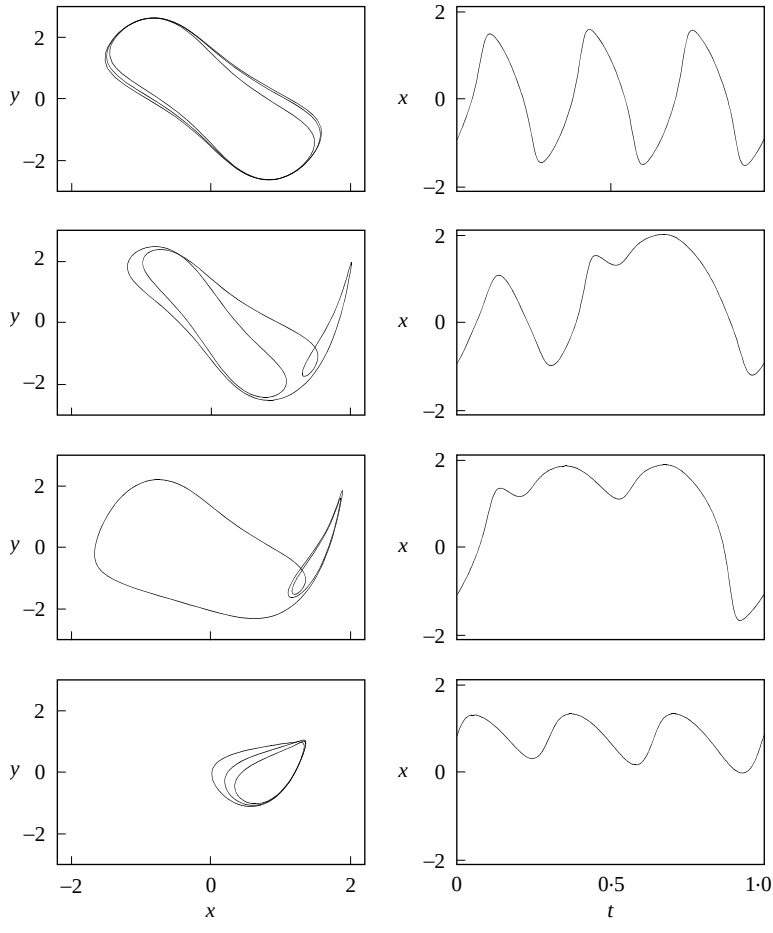

Figure 7. Evolution of the oscillation-sliding phenomenon. Left: projection of the periodic orbits onto the xy plane. Right: x versus t along a normalized period. The values of the parameter v are (up–down): $v = -2{\cdot}119680, -2{\cdot}045187, -1{\cdot}793874, -1{\cdot}041162$ respectively.

In the parameter region where oscillation-sliding is present, other complex dynamical behaviours also occur. Quasiperiodic oscillations (invariant torus), breakdown of the torus and the corresponding resonant periodic orbits have been defined.

Some questions need to be addressed in the near future. In particular, a detailed numerical analysis showing bifurcation diagrams and bifurcation sets of oscillation-sliding periodic orbits will provide important information. Preliminary results (not included in the present paper) suggest the possible relation of this phenomenon to some global bifurcations (homoclinic/heteroclinic connections). A more ambitious and difficult task will be to obtain some analytical information on oscillation-sliding.

ACKNOWLEDGMENTS

This work has been partially supported by the *Comisión Interministerial de Ciencia y Tecnología* (project PB98-1152) and by the *Consejería de Educación y Ciencia de la Junta de Andalucía* (project TIC-0130).

REFERENCES

1. J. GUCKENHEIMER and P. HOLMES 1986 *Nonlinear Oscillations, Dynamical Systems, and Bifurcations of Vector Fields*. Berlin: Springer-Verlag.
2. A. H. NAYFEH, B. BALACHANDRAN 1995 *Applied Nonlinear Dynamics*. New York: Wiley.
3. E. FREIRE, L. G. FRANQUELO and J. ARACIL 1984 *IEEE Transactions on Circuits and Systems CAS* **31**, 237–247. Periodicity and chaos in an autonomous electronic system.
4. A. ALGABA, E. FREIRE, E. GAMERO and A. J. RODRÍGUEZ-LUIS 1998 *Nonlinear Dynamics* **16**, 369–404. Analysis of Hopf and Takens-Bogdanov bifurcations in a modified van der Pol-Duffing Oscillator.
5. A. ALGABA, E. FREIRE, E. GAMERO and A. J. RODRÍGUEZ-LUIS 1999 *International Journal of Bifurcation and Chaos* **9**, 1333–1362. On a codimension-three unfolding of the interaction of degenerate Hopf and pitchfork bifurcations.
6. J. GUCKENHEIMER, M. R. MYERS, F. J. WICKLIN and P. A. WORFOLK 1995 *DSTOOL: A Dynamical System Toolkit with a Interactive Graphical Interface, Reference Manual*. Cornell University: Center for Applied Mathematics.
7. E. DOEDEL, X. WANG, T. FAIRGRIEVE 1995 *AUTO*94, *Software for Continuation and Bifurcation Problems in Ordinary Differential Equations*. Applied Math. Report, CIT.